Microwave antenna design and simulation for dynamic nuclear polarization experiments in semiconductor thin films

Kelley Daenzer[1], J. T. Tokarski, III[2], Dr. C. R. Bowers[2]

1. Department of Physics, University of Colorado at Colorado Springs, Colorado Springs, CO 80918

2. Department of Chemistry, University of Florida, Gainesville, FL 32611

ABSTRACT

Nuclear magnetic resonance (NMR) experiments are powerful and versatile, but they are inherently insensitive due to low polarization at thermal equilibrium. Dynamic nuclear polarization (DNP) is a "hyperpolarization" method that can enhance the NMR sensitivity, enabling experiments on semiconductor thin films and quantum structures. In this REU project, several microwave antenna designs, a horn and a simple dipole antenna, were simulated. Based on the simulations and space constraints of the low temperature cryostat, the geometry and simplicity of the coax-fed dipole antenna was found to be the most appropriate for DNP experiments on semiconductor films at low temperatures (3-5 K). A dipole antenna optimized for 18.5 GHz, fabricated, tested, and integrated into a low-temperature NMR probe. Preliminary data were collected showing a successful DNP effect in the conduction electrons in a GaAs thin film sample.

I. INTRODUCTION

Nuclear magnetic resonance (NMR) is a ubiquitous spectroscopic tool used in chemistry, biology, medicine and physics to gain insight into molecular structure, dynamics, and interesting spin phenomena[1,2]. Despite its versatility, NMR is inherently insenstive[3] due to the small energy differences between spin states in comparison to the available thermal energy (i.e. kT). This leads to small population differences between spin states, also known as low *polarization,* at thermal equilibrium. There are multiple methods to increase the nuclear spin polarization beyond its thermal equilibrium state, leading to what is known as hyperpolarization. When materials become hyperpolarized, the signal intensity will increase, and this allows NMR to investigate much smaller samples, such as thin films of quantum wells or quantum dots. In our work, we will utilize a hyperpolarization technique called dynamic nuclear polarization (DNP). DNP is commonly achieved using a high-power, high-frequency microwave sources[4], such as a gyrotron, which produce a quasi-optical beam of microwaves. However, these can be expensive, cumbersome to operate, and may require other specialized equipment. We propose an alternative microwave system for DNP using a YIG (Yttrium Iron Garnet) source and simple microwave antenna for the study of conduction-electron-nuclear spin interactions in quantum well (QW) thin film of GaAs/AlGaAs. Such quantum confined structures have garnered a lot of attention[5] for possible spintronics and quantum computing purposes. The objective of this NSF/UF Physics REU project was to design and simulate several types of antennas to figure out which would be the best for our experimental setup, to optimize, test and fabricate the antenna. Having met these objectives, the antenna was incorporated into an existing cryogenic NMR probe and demonstrated in preliminary experiments.

II. THEORY

A. NMR and DNP

Nuclei and electrons have intrinsic angular momenta known as “spin”. Spin can be a whole- or half-integer value. This spin value defines the range of allowed values for a particle, ranging from the positive value to the negative value in integer steps. Usually these allowed spin states are indistinguishable, or “degenerate”. However, when the atoms are placed in a magnetic field, the spin states become separated by some energy[3]

$$\Delta E = \frac{h\gamma B}{2\pi}, \tag{1}$$

where ΔE is the energy gap between spin states, B is the external magnetic field, and γ is the gyromagnetic ratio particular to the particle of interest. This phenomenon is called Zeeman splitting. The resonant frequency between states is called the Larmor frequency[3] ν and it can be found by relating equation (1) to Planck’s equation,

$$\Delta E = h\nu . \tag{2}$$

Solve for ν to obtain the Larmor frequency:

$$\nu = \frac{\gamma B}{2\pi}. \tag{3}$$

Typically, at moderate field strengths (3 T) the Larmor frequency is on the order of MHz for nuclei, and GHz for electrons.

A sample is placed in a large external magnetic field, called B_0, and allowed to come to thermal equilibrium, or “relax”. Then a strong radio frequency (RF) pulse with frequency equal to the nuclear Larmor frequency irradiates the sample. The RF pulse will be timed such that the magnetic field of the RF pulse, called the B_1 field, rotates the nuclear magnetization (i.e. the nuclear spins) into the plane perpendicular to the magnetic field. Once the

pulse dissipates and the B_1 field is removed, the spins will want to relax back to the direction of the applied field B_0. They will rotate, or precess, around the axis of the magnetic field. The precessing spins will induce a current in a pickup coil wrapped around the sample, which is measured as a function of time. The signal strength is directly proportional to the polarization of the material. We take the Fourier transform of the signal to obtain the NMR spectrum.

The polarization across a ground state (n_1) and an excited state (n_2) can be approximated in the high temperature limit by following equation[6]

$$\frac{P(n_2)}{P(n_1)} = e^{-\Delta E/kT}, \tag{4}$$

where ΔE is found from equation (1), k is Boltzmann's constant, and T is the temperature in kelvins. At room temperature, ΔE is 3 orders of magnitude smaller than kT and so the population difference between the two nuclear spin states is extremely small – on the order of one part in a million. The net polarization of the sample is small, and so the signal is weak. Researchers overcome this intrinsic insensitivity by using large quantities of sample, larger magnetic fields, very low temperatures, or a combination of the three. However, this is not always accessible to everyone.

To increase the NMR sensitivity, we can utilize DNP. We will focus on Overhauser DNP[4] where an electron has a hyperfine Fermi contact – a quantum mechanical and magnetic interaction between the electron and a nucleus. If a microwave source at the electron's Larmor frequency is directed at the material, the electronic spin states will be excited to a higher energy. Then, by a quantum mechanical process called the Overhauser effect, the electronic and nuclear spins can switch, or "flip-flop" with each other. Thus the nuclear spin state can be excited, thermodynamic concerns can be bypassed, and the sample becomes hyperpolarized. This process

is called dynamic nuclear polarization (DNP). Higher polarization leads to stronger detected signals.

B. Antenna design

1. Horn antennas

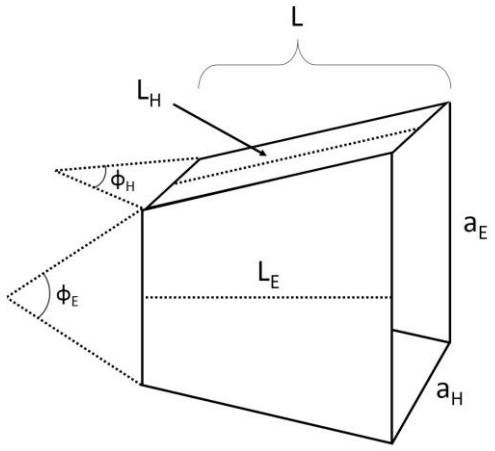

FIG. 1. A horn antenna with labeled sides and angles. a_H and a_E are the aperture width and height, corresponding to the magnetic and electric field, respectively; L_H and L_E are the side lengths of the horn, corresponding to the magnetic and electric field, respectively; L is the total length of the horn; and φ_H and φ_E are the flare angles corresponding to the magnetic and electric field, respectively.

Horn antennas couple electromagnetic waves from inside a waveguide into free space[7]. Their dimensions and flare angle depend on the wavelength used. Additionally, the flare angle of one side will correspond to the electric field of the enclosed light, and those of the other side correspond to the magnetic field. For the most optimal horn, the flare angles for each side are related to the wavelength by

$$\cos\frac{\varphi}{2} = \frac{L/\lambda}{S + L/\lambda}, \tag{5}$$

where φ is the flare angle of either the electric or magnetic field (φ_H or φ_E, respectively), L is the total length of the horn, λ is the wavelength, S_H=0.4 and S_E=0.25 (Ref. 8). The dimensions of the aperture are related to the wavelength by

$$a_E = \sqrt{2\lambda L_E}\,,$$
$$a_H = \sqrt{3\lambda L_H}\,, \tag{6}$$

where L_H and L_E are the lengths of the flared sides[9] and can be calculated using the angle and total length calculated from equation (5). A labeled horn is shown in Fig. 1. The aperture width should be greater than the wavelength of the enclosed light. The aperture height is arbitrary, but it must be less than the aperture width. The horn serves to guide waves into free space with as little distortion as possible. If the surroundings of the wave change too rapidly, there will be distortion around the edges. For this reason, the horn must expand gradually at a flare angle of less than 40 degrees.

2. Dipole antennas

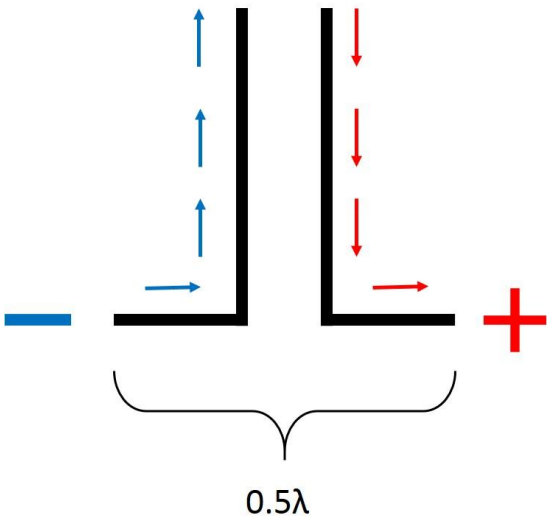

FIG. 2. A dipole antenna. The total length of a perfect half-wave dipole should be ½ the wavelength of interest λ.

Dipole antennas are formed from two conductors parallel to each other on the same axis as shown in Fig. 2. Their length will depend on the desired wavelength. For a perfect half-wave dipole, the total length should be half of the desired wavelength[10]. A half-wave dipole produces a standing wave which radiates isotropically perpendicular to the axis of the two conductors.

III. METHODS & MATERIALS

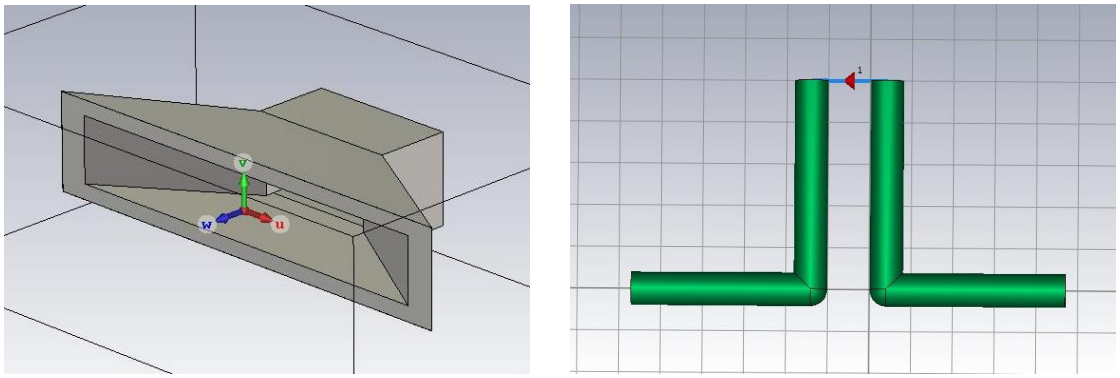

(a) (b)

FIG. 3. (a) 3D model of a horn antenna. (b) 3D model of a dipole antenna.

To select the best antenna design, I used CST Microwave Studio 2017 to digitally build and simulate antennas. 3D CAD models of an antenna are made by generating elemental shapes and defining material parameters. These models are shown in Fig. 3.

The time-domain solver solves Maxwell's equations inside the antenna. It approximates the expectation values throughout the antenna via Finite Element Modelling. The elements are generated from a mesh – a grid with cell sizes determined by the user. An example of this mesh can be seen in Fig. 4.

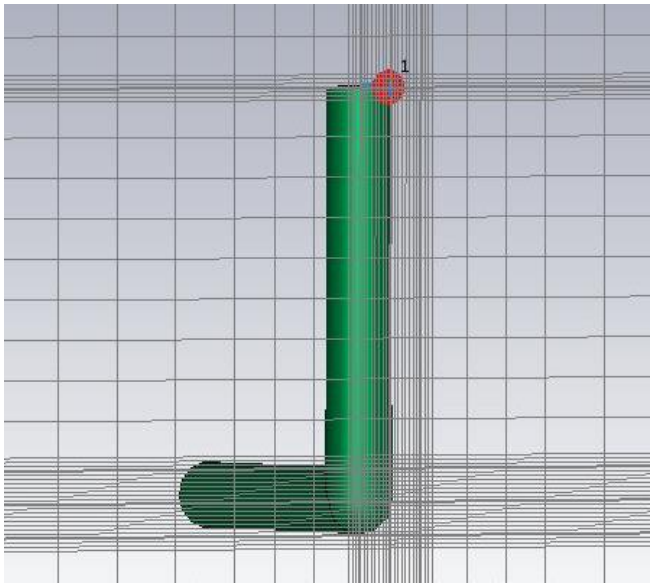

FIG. 4. Mesh view of the dipole antenna.

The simulations provide important information about the antenna, such as the propagation of the electric and magnetic fields and the scattering parameters (S-parameters). Scattering parameters give the relationships between the incident, reflected, and transmitted signals in a system. For systems with multiple ports, the S-parameters are represented by a multi-dimensional square matrix. Our system is a one-port system, so the S-parameter is a one-dimensional square matrix, and represents the ratio of reflected to incident signal. Using the time-domain solver, I simulated data for several iterations of horn and dipole antennas. In many cases it was necessary to sweep various parameters to find the optimum dimensions of the antenna for our specifications.

Once the simulations were complete, we constructed a dipole antenna and the assembly required to operate it. The antenna itself is made from an Anritsu K118 semi-rigid coaxial cable, suitable from 0-46 GHz, terminated at one end by a half-wave dipole antenna. It is placed inside a homebuilt probe. The microwave source is a MicroLambda YIG oscillator being run between 0

V and -2 V to achieve the resonance frequency needed (16.5-18.5 GHz). The YIG is coupled into a DBS Microwave Doubling Amplifier, which both doubles the frequency and amplifies the microwave field. This produces microwaves with a frequency of 18.5 GHz, with a wavelength of approximately 16 mm, which are coupled into the coaxial cable via an Anritsu K-connector. The RF pulse is generated by a Tecmag Scout Spectrometer and amplified by an American Microwave Technologies Linear Amplifier. We used a 3 T Oxford wide bore superconducting magnet. The probe is operated inside an Oxford Continuous Flow Cryostat (CF1200) at 3.8 K. Temperature was monitored at the sample space with a Cernox temperature sensor.

IV. RESULTS & DISCUSSION

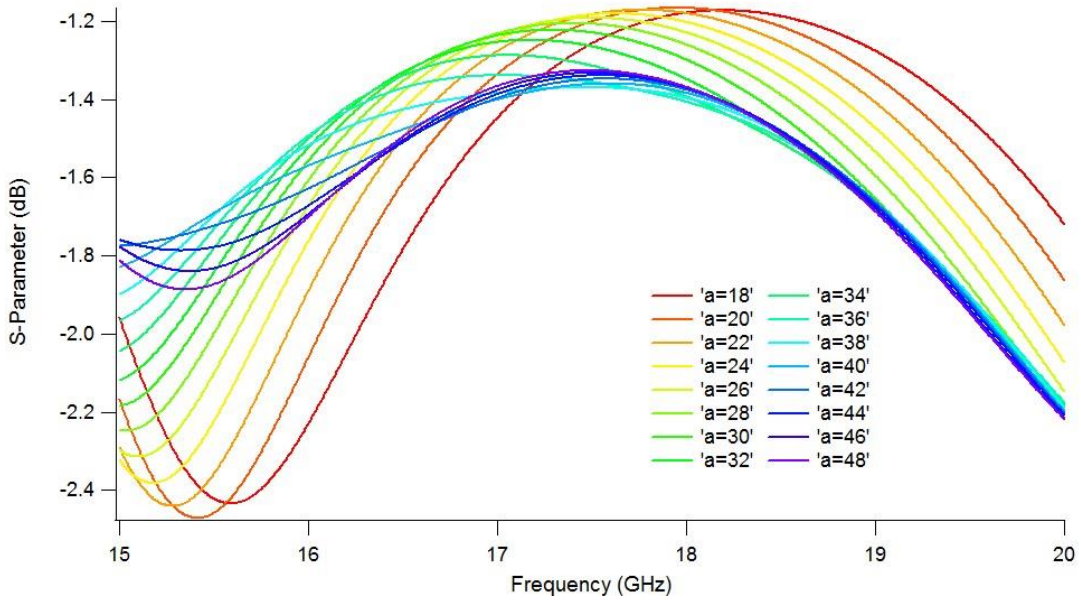

FIG. 5. A graph of S-parameters versus frequency, generated from varying the aperture width of the horn from 18 to 48 mm.

The S-parameters obtained from optimizing the horn aperture width are shown in Fig. 5. Lower scattering occurs for lower values on the graph. As shown in the figure, the least

scattering occurs at a horn width of ~32 mm at 18.5 GHz. This size is impractically large compared to the space available in our probe. Furthermore, the aperture was so much larger than our sample size that the radiated power would have been weak and inefficient.

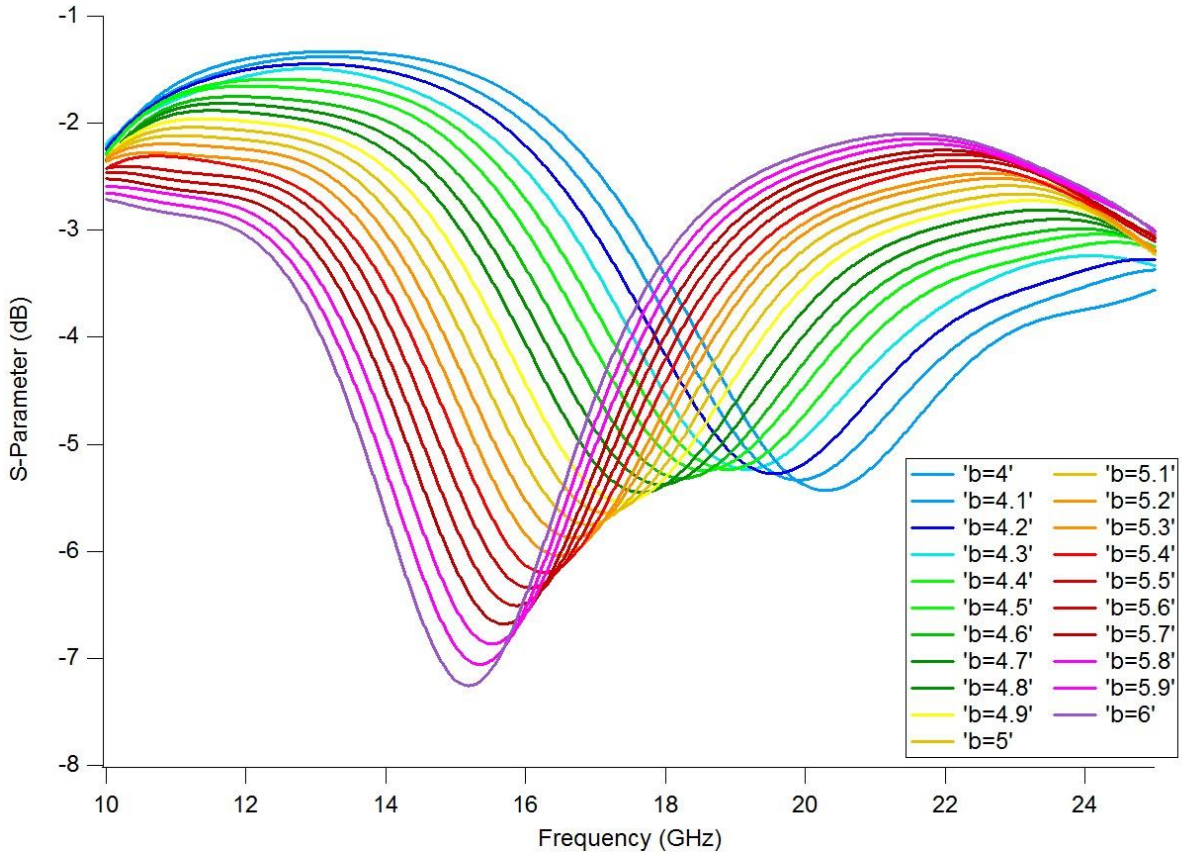

FIG. 6. A graph of S-parameter, measured in decibels, versus frequency, measured in gigahertz; generated by sweeping the length of the dipole legs from 3 to 6 mm (i.e. sweeping the total length of the dipole from 7 to 13 mm).

Figure 6 shows the S-parameters obtained for the dipole antenna. From the figure, it is clear that the optimal length at 18.5 GHz is just over ½ the wavelength of our microwaves (10.5 mm). The dipole antenna takes up far less space inside the probe. However, the radiated power is less intense. It is interesting to note that at higher frequencies, the antenna experiences more scattering. This may be due to an unmatched impedance in the system.

Looking at radiated power, the horn antenna would be ideal because it produces higher power microwaves. However, the beam width of those microwaves is much larger than the sample, so a lot of that power would be wasted. Also, the horn, with its width of 32 mm, is simply too big to fit inside our probe. The dipole antenna, while producing less intense microwaves, can fit easily inside our probe, with a width of only 10.5 mm. Therefore, we determined that the dipole antenna is the best option for our probe.

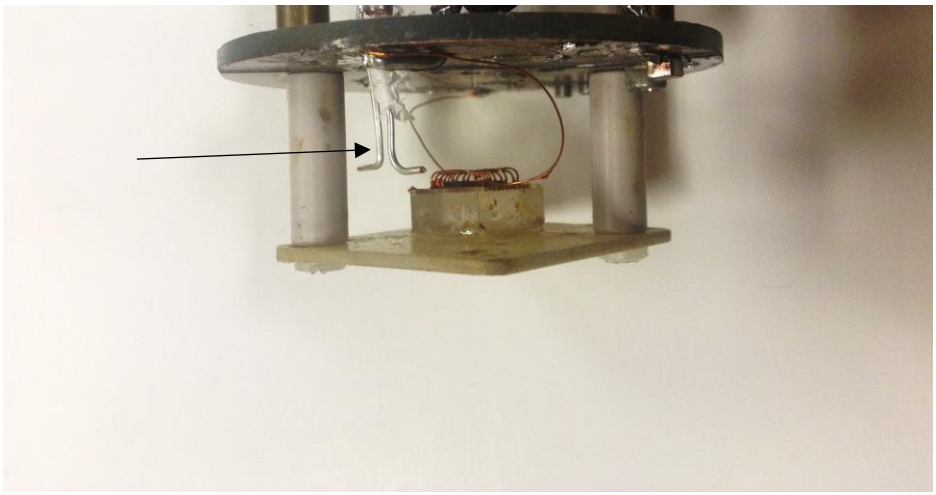

FIG. 7. Microwave antenna installed in the probe, indicated by a black arrow. The copper coil encloses the sample just to the right of the antenna.

Figure 7 shows the dipole antenna installed in the probe. One arm is made directly from the center conductor of the coaxial cable, and the other is made from the same material and soldered to the outer conductor. We implemented what is called a “common-mode choke” by grounding the antenna (i.e. attaching the arm to the outer conductor) several wavelengths away from the antenna arms. Through preliminary testing, we have determined that the antenna is successfully producing microwaves.

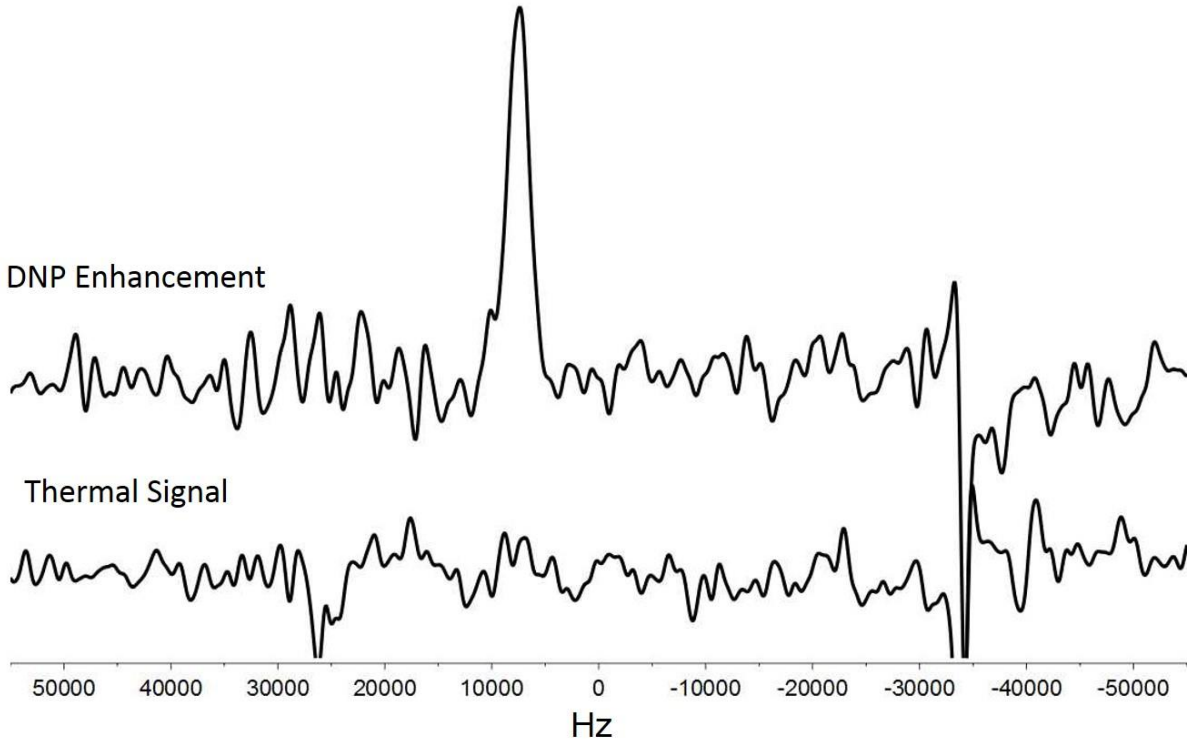

FIG. 8. Preliminary DNP NMR data. The bottom trace shows the thermal signal, i.e. the signal obtained at thermal equilibrium with no microwave radiation. The top trace shows the enhancement achieved by irradiating with microwaves. This signal was acquired at 3 T, 3.8 K, with 200 mW laser power, and with microwaves swept from 17.3-18.5 GHz at a rate of 0.01 GHz min^{-1}.

We acquired DNP NMR with a 30 nm quantum well affixed to a silicon substrate (sample EA124). The previously undetected thin film gave ample signal when irradiated with microwaves and laser light to promote carriers for DNP. As is seen in Fig. 8, we have sizeable enhancement.

V. CONCLUSION

CST Microwave Studio was employed to simulate horn and half-wave dipole antennas at 18.5 GHz. From the simulated antennas, we determined that a half-wave dipole antenna was best suited for our experimental setup. Once we determined this, we constructed the dipole antenna

based on the simulation data and attempted to perform DNP-NMR using it. With further testing, we can fine-tune our antenna so that it works optimally in our probe. Once we fabricated the dipole antenna, we were able to observe signal enhancement in a sample of EA124. Further work will look to optimize the signal, including frequency sweep rate, frequency range, and laser intensity.

ACKNOWLEDGEMENTS

I would like to thank the University of Florida for hosting this REU program, and Dr. Selman Hershfield for coordinating it. I would also like to thank Dr. Russ Bowers, John Tokarski III, and the Bowers Research Group for all their help this summer. This project was funded by NSF DMR-1461019.

REFERENCES

[1]M. Rosay et al., Phys. Chem. Chem. Phys. **12**, 22 (2010).

[2]M. Rosay et al., J. Am. Chem. Soc. **123**, 5 (2001).

[3]James Keeler, *Understanding NMR Spectroscopy* (John Wiley & Sons, West Sussex, 2005), p. 14-47.

[4]T. V. Can et al., J. Chem. Phys. **141**, 6 (2014).

[5]Daniel Loss and David P. DiVincenzo, Phys. Rev. A **57**, 1 (1998).

[6]Daniel V. Schroeder, *An Introduction to Thermal Physics* (Addison Wesley Longman, San Francisco, 2000), p. 223.

[7]Andrew Alford, *Very High-Frequency Techniques*, edited by Herbert J. Reich et al. (Boston Technical Publishers, inc., Cambridge, 1965), p. 1-25; Jessie A. Nelson, David Lazarus, John W. Christensen, and Robert R. Buss, *ibid.*, p. 138-170.

[8]William Sinnema, *Electronic Transmission Technology* (Prentice Hall, Upper Saddle River, 1988), p. 296.

[9]Tasuku Teshirogi, *Modern Millimeter-wave Technologies* (IOS Press, Clifton, 2000), p. 87.

[10]Clayton R. Paul, *Introduction to Electromagnetic Compatibility* (John Wiley & Sons, West Sussex, 2006), p. 433